JACS
JOURNAL OF THE AMERICAN CHEMICAL SOCIETY

ARTICLE

pubs.acs.org/JACS

Synthesis of Cu_2O Nanocrystals from Cubic to Rhombic Dodecahedral Structures and Their Comparative Photocatalytic Activity

Wan-Chen Huang,[†] Lian-Ming Lyu,[†] Yu-Chen Yang,[‡] and Michael H. Huang*[,†]

[†]Department of Chemistry and [‡]Department of Physics, National Tsing Hua University, Hsinchu 30013, Taiwan

Supporting Information

ABSTRACT: In this study, a new series of Cu_2O nanocrystals with systematic shape evolution from cubic to face-raised cubic, edge- and corner-truncated octahedral, all-corner-truncated rhombic dodecahedral, {100}-truncated rhombic dodecahedral, and rhombic dodecahedral structures have been synthesized. The average sizes for the cubes, edge- and corner-truncated octahedra, {100}-truncated rhombic dodecahedra, and rhombic dodecahedra are approximately 200, 140, 270, and 290 nm, respectively. An aqueous mixture of $CuCl_2$, sodium dodecyl sulfate, NaOH, and $NH_2OH \cdot HCl$ was prepared to produce these nanocrystals at room temperature. Simple adjustment of the amounts of $NH_2OH \cdot HCl$ introduced enables this particle shape evolution. These novel particle morphologies have been carefully analyzed by transmission electron microscopy (TEM). The solution color changes quickly from blue to green, yellow, and then orange within 1 min of reaction in the formation of nanocubes, while such color change takes 10−20 min in the growth of rhombic dodecahedra. TEM examination confirmed the rapid production of nanocubes and a substantially slower growth rate for the rhombic dodecahedra. The rhombic dodecahedra exposing only the {110} facets exhibit an exceptionally good photocatalytic activity toward the fast and complete photodegradation of methyl orange due to a high number density of surface copper atoms, demonstrating the importance of their successful preparation. They may serve as effective and cheap catalysts for other photocatalytic reactions and organic coupling reactions.

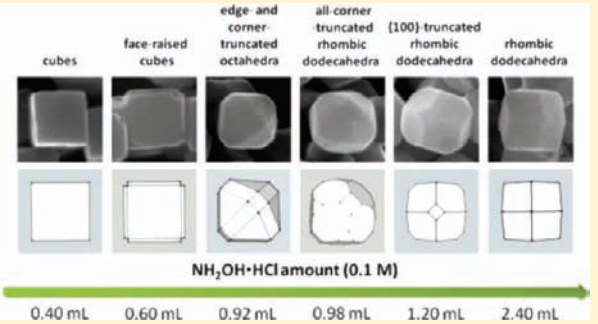

INTRODUCTION

The growth of inorganic nanocrystals with cubic, octahedral, and rhombic dodecahedral structures is interesting not only because facet-dependent catalytic, photocatalytic, electrical, and molecular adsorption properties can be investigated with greater certainty, but also because the synthetic conditions used to achieve such shape evolution may provide insights into factors controlling the particle morphology.[1−15] In addition, novel intermediate nanocrystal structures may be obtained if the synthetic route yields particles with systematic shape evolution. Previously, we have demonstrated one-pot synthesis of cuprous oxide (Cu_2O) nanocrystals with systematic shape evolution from cubic to cuboctahedral and octahedral structures in aqueous solution.[16,17] The rhombic dodecahedron represents another important Cu_2O nanocrystal morphology to synthesize because facet-dependent property investigations of Cu_2O crystals can be extended to the {110} faces. Their growth conditions can be compared with those of cubic and octahedral particles to gain mechanistic insights if the synthetic procedure allows systematic shape evolution from these particle structures. Gao et al. first reported the synthesis of rhombic dodecahedral microcrystals by heating aqueous $CuSO_4$, oleic acid, ethanol, NaOH, and D-(+)-glucose to 100 °C for 1 h.[18] Zeng and co-workers reacted copper(II) acetate, hexadecylamine, and undecane at 160−220 °C for 15−90 min to form Cu_2O nanocrystals with sizes of ∼70 nm.[19] Hexadecylamine was believed to play multiple roles as a ligand, phase-transfer agent, reducing agent, and surface-regulating agent. Zhang et al. synthesized Cu_2O rhombic dodecahedral microcrystals by mixing $Cu(NO_3)_2$, formic acid, and NH_3 in an ethanol−water mixture hydrothermally at 145 °C for 90 min.[20] All of these methods suffer from the use of high temperatures. Employment of different amounts of oleic acid and hexadecylamine as capping agents to control the particle morphology is more difficult to rationalize. It would be desirable to develop a simple synthetic approach to make Cu_2O rhombic dodecahedra at room temperature using reaction conditions similar to those previously developed to prepare Cu_2O nanocubes and octahedra.[16,17]

In this study, we have synthesized a new series of Cu_2O nanocrystals with systematic shape evolution from cubic to rhombic dodecahedral structures at room temperature by mixing an aqueous solution of $CuCl_2$, sodium dodecyl sulfate (SDS) surfactant, NaOH, and $NH_2OH \cdot HCl$ reductant. Novel intermediate particle morphologies were synthesized. Their structures have been extensively characterized and confirmed. The growth processes of nanocubes and rhombic dodecahedra have been studied by following the remarkable solution color changes and examining the particles formed at the early growth stage. Finally, the Cu_2O

Received: October 14, 2011
Published: December 14, 2011

dx.doi.org/10.1021/ja209662v | J. Am. Chem. Soc. 2012, 134, 1261–1267

rhombic dodecahedra were used as catalysts for the photodegradation of methyl orange. They displayed significantly better photocatalytic activity than Cu_2O octahedra and cubes, demonstrating the importance of making the rhombic dodecahedra. They can be examined for facet-dependent electrical and catalytic properties with cubes and octahedra.[21,22]

EXPERIMENTAL SECTION

Chemicals. Anhydrous copper(II) chloride ($CuCl_2$; 97%) and hydroxylamine hydrochloride ($NH_2OH \cdot HCl$; 99%) were purchased from Aldrich. Sodium hydroxide (98.2%) and SDS (100%) were acquired from Mallinckrodt. All chemicals were used as received without further purification. Ultrapure distilled and deionized water (18.3 MΩ) was used for all solution preparations.

Cu_2O Nanocrystal Synthesis. For the synthesis of Cu_2O nanocrystals with systematic shape evolution from cubic to rhombic dodecahedral structures, 8.92, 8.72, 8.40, 8.34, 8.12, and 6.92 mL of deionized water were respectively added to sample vials labeled a, b, c, d, e, and f. The sample vials were placed in a water bath set at 32−34 °C. Then 0.5 mL of 0.1 M $CuCl_2$ solution and 0.087 g of SDS powder were added to each vial with vigorous stirring. After complete dissolution of SDS powder, 0.18 mL of 1.0 M NaOH solution was introduced. The resulting solution turned light blue immediately, indicating the formation of $Cu(OH)_2$ precipitate. Finally, 0.40, 0.60, 0.92, 0.98, 1.20, and 2.40 mL of 0.1 M $NH_2OH \cdot HCl$ were quickly injected in 5 s into vials a, b, c, d, e, and f, respectively. The total solution volume in each vial is 10 mL. The vials were stirred for 20 s. The concentrations of Cu^{2+} ions and SDS surfactant in the final solution were 1.0×10^{-3} and 3.0×10^{-2} M, respectively. The solutions were kept in the water bath for 1 h for nanocrystal growth and centrifuged at 5000 rpm for 3 min. After the top solution was decanted, the precipitate was washed with 6 mL of a 1:1 volume ratio of water and ethanol. The precipitate was centrifuged and washed again using the same water/ethanol mixture to remove unreacted chemicals and SDS surfactant. The final washing step used 5 mL of ethanol, and the precipitate was dispersed in 0.6 mL of ethanol for storage and analysis.

Photocatalysis Experiments. For the photocatalytic activity measurements, a 10-fold reagent amount of the synthesized Cu_2O nanocrystals was used. Thus, the total solution volume was increased to 100 mL in the synthesis of the Cu_2O nanocrystals. Nanocubes and rhombic dodecahedra were selected for their comparative photocatalytic activity investigation. The entire centrifuged Cu_2O nanocrystals were dispersed in 90 mL of 30 mg/L aqueous methyl orange solution. The entire solution was transferred to a homemade cubic quartz cell with an inner cell edge length of about 4.5 cm and a small capped opening at the top. Before illumination, the cell was constantly stirred for 30 min in the dark for the molecules to adsorb onto the particle surfaces. After that the cell was irradiated with light from a 500 W xenon lamp placed 28 cm away. The light intensity reaching the cell was measured to be 500 mW/cm^2 using a power meter. UV−vis absorption spectra of the samples were taken before and after every 10 min of irradiation for up to 90 min by removing the cap to withdraw the solution.

Instrumentation. Scanning electron microscopy (SEM) images of the synthesized nanocrystals were obtained using a JEOL JSM-7000F scanning electron microscope. Transmission electron microscopy (TEM) characterization was performed on a JEOL JEM-2100 electron microscope operating at 200 kV. Powder X-ray diffraction (XRD) patterns were collected using a Shimadzu XRD-6000 diffractometer with Cu Kα radiation. UV−vis absorption spectra were acquired with the use of a JASCO V-570 spectrophotometer. The Cu_2O crystal structures were drawn using the Google SketchUp 7 program.

RESULTS AND DISCUSSION

Previously, {100}-truncated rhombic dodecahedral Cu_2O nanocages were fabricated by mixing deionized water, $CuCl_2$, SDS surfactant, $NH_2OH \cdot HCl$, HCl, and NaOH in the order listed.[23] We considered this synthetic method a good starting point to prepare Cu_2O rhombic dodecahedra. Since HCl was purposely added as an etchant, it does not seem necessary to introduce HCl for the growth of solid Cu_2O particles. Actually, the solution pH can drop from the following reactions:

$$CuCl_2 + 6H_2O \leftrightarrow Cu(H_2O)_6^{2+} + 2Cl^- \quad (1)$$

$$Cu(H_2O)_6^{2+} \leftrightarrow [Cu(H_2O)_5(OH)]^+ + H^+ \quad (2)$$

If a slightly acidic solution condition is favorable for the formation of rhombic dodecahedra, such a condition can be achieved by increasing the amount of $CuCl_2$ used without adding HCl. In this study, the volume of 0.1 M $CuCl_2$ solution added is 0.5 mL instead of the 0.1 mL previously used, and the NaOH volume is decreased to 0.18 mL from the 0.20 mL used before. By varying the volumes of $NH_2OH \cdot HCl$ reductant introduced over a wide range from 0.40 to 2.40 mL, a series of Cu_2O nanostructures from nanocubes to rhombic dodecahedra were synthesized. Scheme S1 in the Supporting Information gives a summary of the reaction conditions used. Figure 1 shows the SEM images of the Cu_2O nanocrystals synthesized. By progressively increasing the volumes of $NH_2OH \cdot HCl$ added, cubes, face-raised cubes, edge- and corner-truncated octahedra, all-corner-truncated rhombic dodecahedra, {100}-truncated rhombic dodecahedra, and finally rhombic dodecahedra were synthesized. Thus, in addition to the successful preparation of Cu_2O rhombic dodecahedra, several interesting intermediate nanostructures were obtained. Figure 2 provides the SEM images of each particle shape viewed from two different orientations. Each {100}-truncated rhombic dodecahedron has six square {100} faces in addition to twelve {110} facets. If the shared corner of three adjacent rhombic faces forms a flat {111} face, a {100}-truncated rhombic dodecahedron becomes an all-corner-truncated rhombic dodecahedron. There are eight triangular {111} faces in an all-corner-truncated rhombic dodecahedron. It is structurally related to the edge- and corner-truncated octahedra. The face-raised cubes have protruded {100} faces. The average particle sizes for the cubes, edge- and corner-truncated octahedra, {100}-truncated rhombic dodecahedra, and rhombic dodecahedra are 202, 142, 273, and 290 nm with standard deviations of 10% or less (see Figure S1 and Table S1 in the Supporting Information for the particle size histograms and standard deviations). This is the first time Cu_2O rhombic dodecahedra with sizes of around 300 nm have been synthesized. Parts c−e of Figure 1 reveal that some nanocrystals exhibit small depressions on their surfaces. This occurs presumably due to the acidic solution condition used during particle synthesis.[23,24] The solution pH decreases from 10.70 for the Cu_2O nanocubes to 6.56 for the edge- and corner-truncated octahedra, 6.22 for the all-corner-truncated rhombic dodecahedra, 5.73 for the {100}-truncated rhombic dodecahedra, and 5.35 for the rhombic dodecahedra. The results show the reaction mixture going from basic to acidic with increasing amounts of $NH_2OH \cdot HCl$ added.

The identity and detailed crystal structures of these Cu_2O nanocrystals were analyzed using XRD and TEM characterization. XRD patterns of these nanocrystals match that of Cu_2O (see Figure S2 in the Supporting Information). Although their XRD patterns look similar due to random particle orientations on

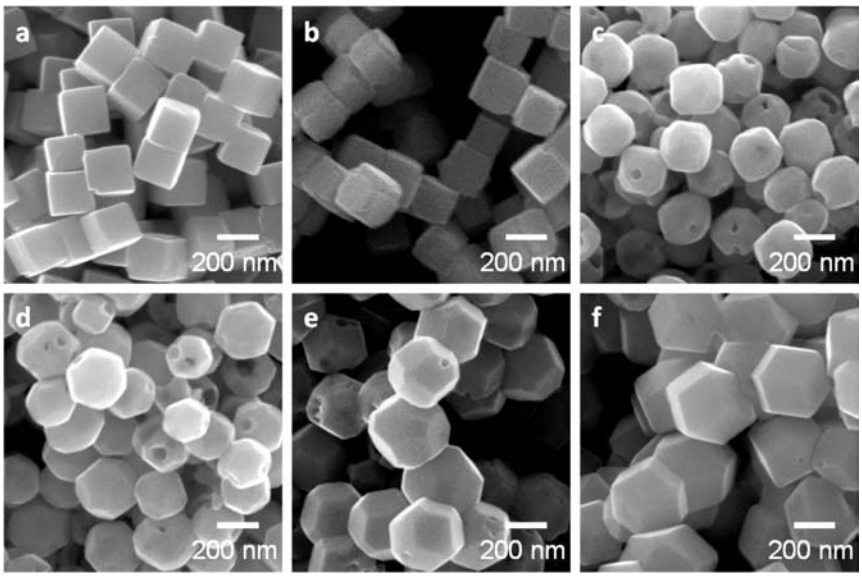

Figure 1. SEM images of the Cu_2O nanocrystals synthesized with various morphologies: (a) cubes, (b) face-raised cubes, (c) edge- and corner-truncated octahedra, (d) all-corner-truncated rhombic dodecahedra, (e) {100}-truncated rhombic dodecahedra, and (f) rhombic dodecahedra.

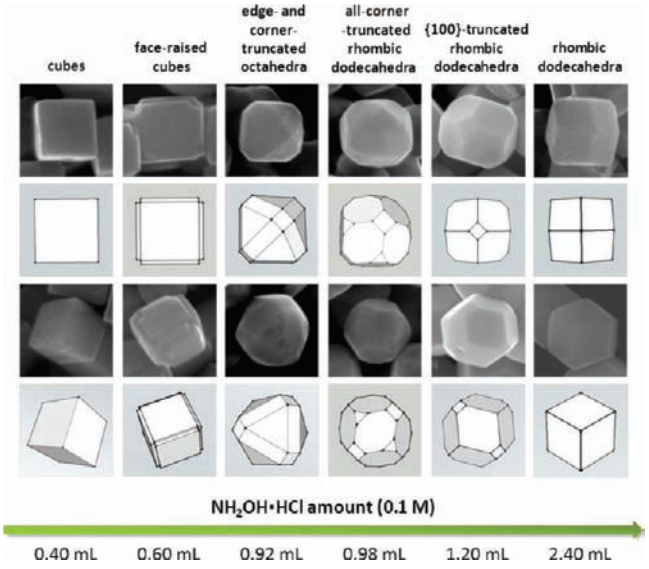

Figure 2. SEM images and the corresponding schematic drawings of the Cu_2O nanocrystals synthesized with morphology evolution from cubes to rhombic dodecahedra upon increasing the amount of $NH_2OH \cdot HCl$ added to the reaction mixture. Two orientations are shown for each particle shape.

a substrate, a close examination shows that the ratio of the intensity of the (220) peak to that of the (200) peak increases from 0.36 for the cubes to 0.6, 0.7, and 0.79 for the edge- and corner-truncated octahedra, {100}-truncated rhombic dodecahedra, and rhombic dodecahedra, respectively. This trend is expected considering the growing fractions of {110} faces. To further confirm the morphologies of new Cu_2O nanostructures synthesized, a detailed TEM analysis has been performed on the edge- and corner-truncated octahedra, all-corner-truncated rhombic dodecahedra, and rhombic dodecahedra. Figure 3 gives the TEM images, selected-area electron diffraction (SAED) patterns, and high-resolution TEM images of Cu_2O edge- and corner-truncated octahedra viewed along the [100], [110], and [111] directions. Representative drawings of the particles showing the same orientations as those seen in the TEM images are also provided. The SAED patterns match the respective orientations of the edge- and corner-truncated octahedra. The high-resolution TEM images taken near the particle edges reveal distinct lattice fringes with *d* spacings of 2.4 and 2.9 Å, which correspond to the (111) and (110) lattice planes of Cu_2O. The lattice plane directions are also consistent with the respective particle orientation. Figure 4 presents the TEM images and the corresponding SAED patterns of rhombic dodecahedra viewed along the [100], [110], and [111] directions. Drawings showing each particle orientation are also included. Again the SAED patterns obtained are consistent with the respective particle orientations and the particle surfaces bound by the {110} facets. Similar TEM images, SAED patterns, and high-resolution TEM images of all-corner-truncated rhombic dodecahedra viewed along the [100] and [110] directions are offered in Figure S3 in the Supporting Information. The analysis also verifies their geometries. The small {111} surface area on these nanocrystals means that finding an isolated all-corner-truncated rhombic dodecahedron positioned along the [111] zone axis is unlikely.

The optical properties of selected Cu_2O nanocrystals synthesized have been studied by obtaining UV−vis absorption spectra of the final products (see Figure S4 in the Supporting Information). Cubes, {100}-truncated rhombic dodecahedra, and rhombic dodecahedra have sizes of 200−300 nm and display characteristic light scattering features from 500 to 1300 nm and a small absorption band at 440−450 nm. The edge- and corner-truncated octahedra have sizes of just ∼140 nm, so a single light scattering band appears at 540 nm. An interesting observation made during nanocrystal growth is a series of changes in the solution color. Immediately after addition of NaOH to the aqueous mixture of $CuCl_2$ and SDS, the solution was light blue from the formation of $Cu(OH)_2$ and possibly $Cu(OH)_4^{2-}$ species. In the synthesis of Cu_2O nanocubes, the solution color turned from light blue to green within seconds after the introduction of $NH_2OH \cdot HCl$ to start nanocrystal growth (see Figure S5 in the

dx.doi.org/10.1021/ja209662v | *J. Am. Chem. Soc.* 2012, 134, 1261–1267

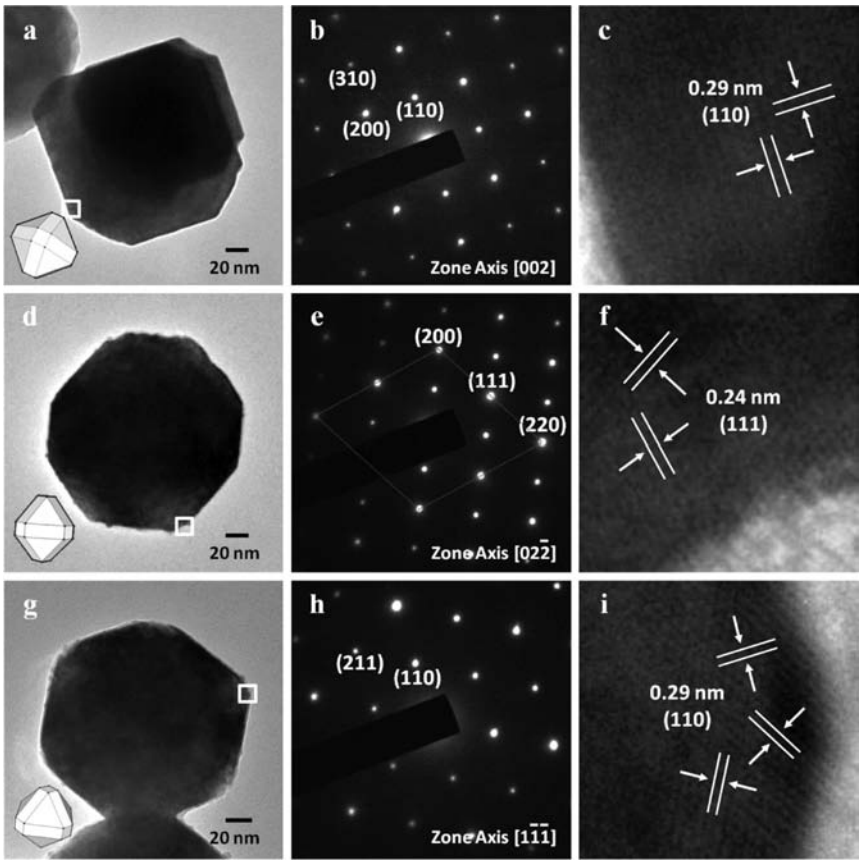

Figure 3. TEM images, SAED patterns, and high-resolution TEM images of the square regions of Cu_2O edge- and corner-truncated octahedra viewed along the (a−c) [100], (d−f) [110], and (g−i) [111] directions. In panel a, a truncated octahedron sits on top of another octahedron having the same orientation.

Supporting Information). The solution color was green-yellow after 20 s of reaction and deep yellow or orange in color after 40 s of reaction. No obvious further change in the solution color was observed. Since Cu_2O nanocrystals in the 200−300 nm size range exhibit this color, the observation implies that the growth rate of nanocubes is quite fast. Similar solution color changes were also observed in the synthesis of Cu_2O rhombic dodecahedra, but the evolution proceeded at a much slower rate. The solution was still green after 3 min of reaction, yellow between 8 and 10 min, and orange from 10 to 60 min of reaction (see Figure 5 and Figure S6 in the Supporting Information). This observation therefore suggests a much slower growth rate in the formation of rhombic dodecahedra. Thus, an important insight from this observation is that the production of different Cu_2O nanocrystal geometries is highly related to their different growth rates. UV−vis absorption spectra in the synthesis of Cu_2O rhombic dodecahedra have been recorded (see Figure 5). Between 1 and 8 min, a strong absorption band centered at 402−404 nm was recorded due to the small particle sizes. The appearance of a light scattering feature at 8 min indicates an increase in the particle size. Multiple light scattering bands dominate in the spectra of rhombic dodecahedra from 15 to 60 min as particles grow larger. From the light scattering features, the nanocrystals should have reached their final dimensions after 30 min of reaction. The absorption band shifts from 410 nm at 15 min to 446 nm at the end of reaction. Due to the extremely rapid changes of solution color, time-dependent absorption spectra were not obtained for the nanocubes.

To further probe the nanocube growth process, particles formed at the early stage were analyzed (see Figure 6). Remarkably, cubes have already been formed in just 30 s after the addition of $NH_2OH\cdot HCl$, a result consistent with the observed solution color. Some fibrous materials can be seen surrounding the nanocubes, which are believed to be $Cu(OH)_2$ structures. The nanocubes grew larger from ~170 nm at 30 s to 200 nm after 1 min with rough surfaces. Cubes with flat faces should form after a period of surface reconstruction.[16] The growth process for the rhombic dodecahedra was also examined (see Figures S7 and S8 in the Supporting Information). Nanoparticles formed upon addition of NaOH to the aqueous mixture of $CuCl_2$ and SDS were confirmed to be $Cu(OH)_2$. A lattice fringe spacing of 0.26 nm corresponding to the (002) lattice planes of $Cu(OH)_2$ was measured. One minute after the introduction of $NH_2OH\cdot HCl$, only tiny Cu_2O nanoparticles with sizes of less than 10 nm were observed. Spherical Cu_2O particles ~40 nm in size and with a polycrystalline nature were found after 2 min of reaction. A quasi-rhombic dodecahedron ~75 nm in size was identified after 3 min of reaction. The results clearly show that, after 1 min of reaction, nanocubes have reached their final dimensions, but rhombic dodecahedra are far from their final sizes after 3 min of particle growth. Considering a much larger amount of $NH_2OH\cdot HCl$ reductant added in the synthesis of rhombic dodecahedra than that used for the formation of nanocubes, one might think the growth rate for the rhombic dodecahedra should be faster. However, rhombic dodecahedra are grown in an acidic solution

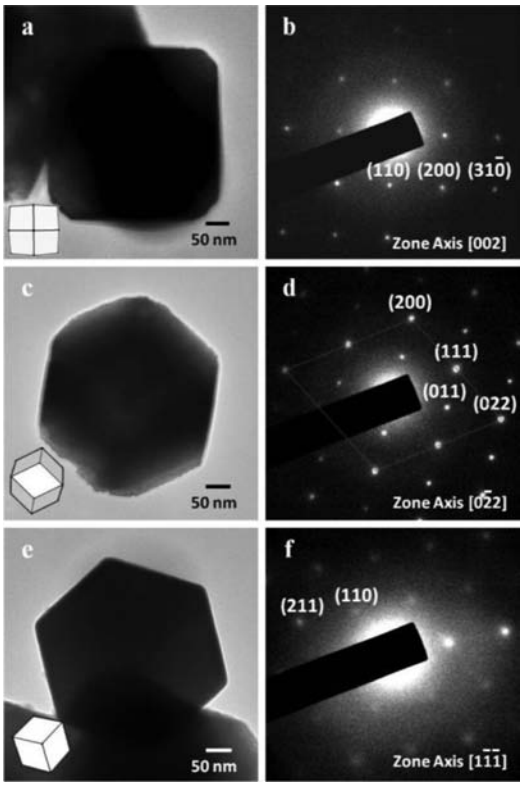

Figure 4. TEM images of Cu_2O rhombic dodecahedra viewed along the (a) [100], (c) [110], and (e) [111] directions and their corresponding SAED patterns.

condition. Etching of Cu_2O by reaction with HCl (from $NH_2OH \cdot HCl$) and/or oxidation of Cu_2O may occur via the following reaction with a standard reduction potential of 1.23 V:

$$O_2 + 4H^+ + 4e^- \rightarrow 2H_2O \quad (3)$$

This should slow the overall reaction rate in the growth of rhombic dodecahedra and also explains the slow formation of truncated rhombic dodecahedral nanocages (2 h) reported previously.[23] The two reactions should not happen in the growth of Cu_2O nanocubes at pH 10.70. Finally, it is worth noting that preferential adsorption of SDS molecules on certain planes cannot be used to explain the produced nanocrystal shapes because both cubes and rhombic dodecahedra with exclusive surface planes (that is, {100} faces vs {110} faces) were synthesized using the same amount of surfactant.

The successful preparation of rhombic dodecahedra offers the opportunity to extend the facet-dependent photocatalytic activity investigation of Cu_2O nanocrystals to the {110} faces. Previously, we have shown that sharp-faced Cu_2O cubes bound exclusively by the {100} faces are inactive toward the photodegradation of methyl orange, a molecule carrying a negative charge, while Cu_2O octahedra exhibit a moderate activity.[14,17] In one study, the fraction of remaining methyl orange absorbance after irradiation of Cu_2O octahedra for 240 min is 64% at 10-fold the normal reagent amount used for the synthesis of Cu_2O octahedra and a methyl orange concentration of 15 mg/L in 90 mL of solution.[17] In another study, the remaining methyl orange absorbance after irradiation of Cu_2O octahedra for 240 min is 65.6% at 20-fold the normal reagent amount used for the synthesis of Cu_2O octahedra and the same methyl orange concentration.[14] Figure 7 gives a

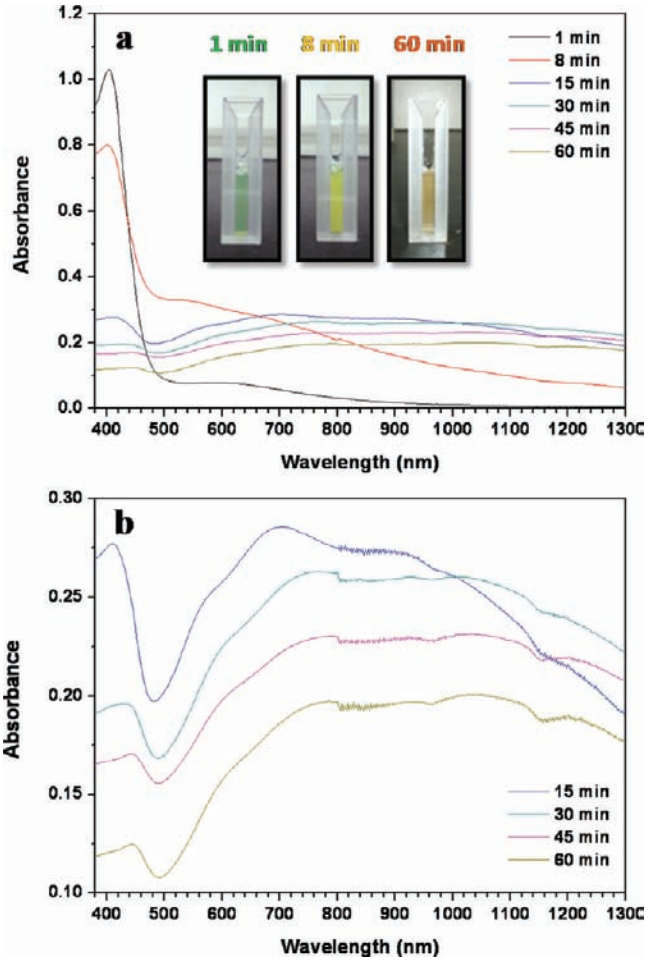

Figure 5. (a) UV−vis spectra of the rhombic dodecahedral products obtained at different reaction times. The Cu_2O particle absorption band maxima are located at 402, 404, 410, 430, 444, and 446 nm at reaction times of 1, 8, 15, 30, 45, and 60 min, respectively. The inset shows photographs of the cuvettes at different reaction times. (b) Enlarged spectra for the reaction times from 15 to 60 min.

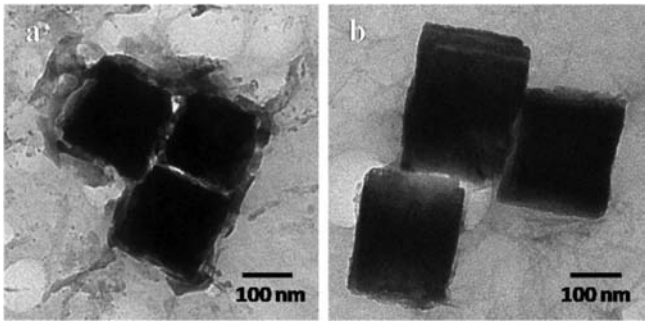

Figure 6. TEM images of Cu_2O nanocubes collected after (a) 30 s and (b) 1 min of reaction following the addition of $NH_2OH \cdot HCl$.

plot of the extent of photodegradation of methyl orange vs time using rhombic dodecahedral and cubic Cu_2O nanocrystals as the photocatalysts. The corresponding UV−vis absorption spectra are available in Figure S9 in the Supporting Information. The cubes are essentially inactive as observed before. The slight degree of photodegradation recorded may be attributed to the imperfect

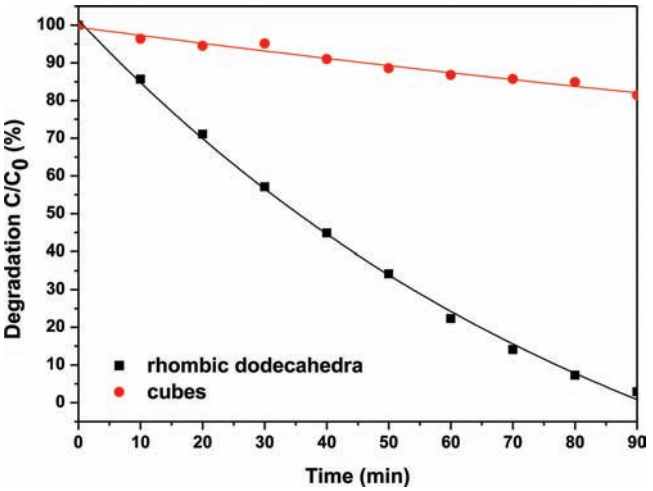

Figure 7. Extent of photodegradation of methyl orange vs time using rhombic dodecahedral and cubic Cu_2O nanocrystals as the photocatalysts.

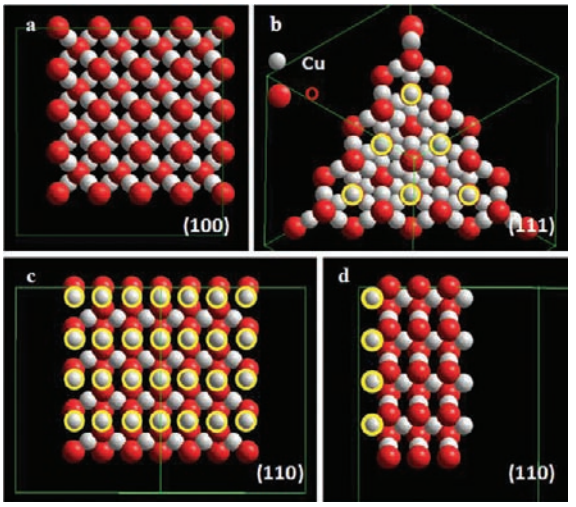

Figure 8. Crystal structures of Cu_2O oriented to show the (a) (100), (b) (111), and (c, d) (110) planes. Surface Cu atoms on the {110} and {111} faces are shown with yellow circles.

cubic shapes for some nanocrystals as seen in Figure 1, which may contain some non-{100} faces. Another possibility is that some nanocubes may stick to the top of the cell wall along with adsorbed methyl orange molecules during stirring of the solution. The inactivity can be further validated since there are periods with barely any decrease in the absorbance of methyl orange (for example, between 10 and 30 min) despite continuous photoirradiation. On the contrary, methyl orange is almost completely photodecomposed by Cu_2O rhombic dodecahedra after 90 min of photoirradiation. Such superb photocatalytic performance has not been measured for Cu_2O nanocrystals. The results show that rhombic dodecahedral Cu_2O nanocrystals bound exclusively by the {110} faces may potentially be excellent photocatalysts for many other reactions. High photocatalytic activity of the {110} surfaces has been suggested using Cu_2O microcrystals exposing significant {110} facets.[25] After the reaction, the initial orange solution became almost colorless after the Cu_2O nanocrystals settled to the bottom of the cell (see Figure S10 in the Supporting Information). When the rhombic dodecahedra were dispersed in a methylene blue solution, they floated to the top of the solution after the solution was stirred for 30 min (see Figure S10). This behavior is similar to that observed for Cu_2O and Ag_2O octahedra and hexapods bound by the {111} facets.[8,17] This effect has been attributed to the electrostatic repulsion interactions between the copper atom-terminated {111} faces of Cu_2O and the positively charged methylene blue molecules. Figure 8 displays crystal structures of Cu_2O oriented to show the (100), (111), and (110) planes. The terminal copper atoms have been highlighted with yellow circles. The number of terminal copper atoms per unit surface area on the {110} face is roughly 1.5 times higher than that found on the {111} face. The {110} face is likely more positively charged compared to the {111} face, while the {100} face is relatively neutral.[17] This should greatly increase the number of methyl orange molecules adsorbed onto the {110} faces and explain the significantly higher photocatalytic activity of the rhombic dodecahedra. The same electrostatic repulsive interactions between the {110} surfaces of rhombic dodecahedra and methylene blue molecules also account for the observed phenomenon of floating nanocrystals.

CONCLUSION

In this study, we have achieved a new series of Cu_2O nanocrystal synthesis with systematic morphology evolution from cubic to rhombic dodecahedral structures with sizes of largely 200−300 nm. Unusual particle shapes such as edge- and corner-truncated octahedral and {100}-truncated rhombic dodecahedral structures were also synthesized. Their structures have been extensively analyzed. The nanocubes were found to grow rapidly within 1 min, while the growth rate for the rhombic dodecahedra was appreciably slower. This difference in growth rate is related to the difference in solution pH. Cu_2O rhombic dodecahedra exhibit exceptionally good photocatalytic activity, demonstrating the importance of their successful preparation. They should hold promise as excellent and cheap catalysts for many other reactions, including organic coupling reactions.

ASSOCIATED CONTENT

Supporting Information. Schematic illustration of the synthetic procedure, size distribution histograms, XRD patterns, additional TEM characterization of Cu_2O nanocrystals and intermediate particles, UV−vis absorption spectra of different nanocrystals, time-resolved photographs of the solutions during particle growth, time-dependent UV−vis spectra and photographs of the photoirradiated methyl orange solution, and a photograph of rhombic dodecahedra suspended in a methylene blue solution. This material is available free of charge via the Internet at http://pubs.acs.org.

AUTHOR INFORMATION

Corresponding Author
hyhuang@mx.nthu.edu.tw

ACKNOWLEDGMENT

We thank the National Science Council of Taiwan for the support of this work (Grant NSC 98-2113-M-007-005-MY3).

REFERENCES

(1) Wu, H.-L.; Tsai, H.-R.; Hung, Y.-T.; Lao, K.-U.; Liao, C.-W.; Chung, P.-J.; Huang, J.-S.; Chen, I.-C.; Huang, M. H. *Inorg. Chem.* **2011**, *50*, 8106–8111.

(2) Bi, Y.; Ouyang, S.; Umezawa, N.; Cao, J.; Ye, J. *J. Am. Chem. Soc.* **2011**, *133*, 6490–6492.

(3) Kuo, C.-H.; Yang, Y.-C.; Gwo, S.; Huang, M. H. *J. Am. Chem. Soc.* **2011**, *133*, 1052–1057.

(4) Read, C. G.; Steinmiller, E. M. P.; Choi, K.-S. *J. Am. Chem. Soc.* **2009**, *131*, 12040–12041.

(5) Chen, Y.-X.; Chen, S.-P.; Zhou, Z.-Y.; Tian, N.; Jiang, Y.-X.; Sun, S.-G.; Ding, Y.; Wang, Z. L. *J. Am. Chem. Soc.* **2009**, *131*, 10860–10862.

(6) Bratlie, K. M.; Lee, H.; Komvopoulos, K.; Yang, P.; Somorjai, G. A. *Nano Lett.* **2007**, *7*, 3097–3101.

(7) Wang, J.; Gong, J.; Xiong, Y.; Yang, J.; Gao, Y.; Liu, Y.; Lu, X.; Tang, Z. *Chem. Commun.* **2011**, *47*, 6894–6896.

(8) Lyu, L.-M.; Wang, W.-C.; Huang, M. H. *Chem.—Eur. J.* **2010**, *16*, 14167–14174.

(9) Chung, P.-J.; Lyu, L.-M.; Huang, M. H. *Chem.—Eur. J.* **2011**, *17*, 9746–9752.

(10) Wu, H.-L.; Kuo, C.-H.; Huang, M. H. *Langmuir* **2010**, *26*, 12307–12313.

(11) Kuo, C.-H.; Huang, M. H. *Nano Today* **2010**, *5*, 106–116.

(12) Huang, M. H.; Lin, P.-H. *Adv. Funct. Mater.* **2012**, DOI: 10.1002/adfm.201101784.

(13) Kuo, C.-H.; Hua, T.-E.; Huang, M. H. *J. Am. Chem. Soc.* **2009**, *131*, 17871–17878.

(14) Wang, W.-C.; Lyu, L.-M.; Huang, M. H. *Chem. Mater.* **2011**, *23*, 2677–2684.

(15) Niu, W.; Zhang, L.; Xu, G. *ACS Nano* **2010**, *4*, 1987–1996.

(16) Kuo, C.-H.; Huang, M. H. *J. Phys. Chem. C* **2008**, *112*, 18355–18360.

(17) Ho, J.-Y.; Huang, M. H. *J. Phys. Chem. C* **2009**, *113*, 14159–14164.

(18) Liang, X.; Gao, L.; Yang, S.; Sun, J. *Adv. Mater.* **2009**, *21*, 2068–2071.

(19) Yao, K. X.; Yin, X. M.; Wang, T. H.; Zeng, H. C. *J. Am. Chem. Soc.* **2010**, *132*, 6131–6144.

(20) Lan, X.; Zhang, J.; Gao, H.; Wang, T. *CrystEngComm* **2011**, *13*, 633–636.

(21) Kim, J. Y.; Park, J. C.; Kim, A.; Kim, A. Y.; Lee, H. J.; Song, H.; Park, K. H. *Eur. J. Inorg. Chem.* **2009**, 4219–4223.

(22) Colacino, E.; Villebrun, L.; Martinez, J.; Lamaty, F. *Tetrahedron* **2010**, *66*, 3730–3735.

(23) Kuo, C.-H.; Huang, M. H. *J. Am. Chem. Soc.* **2008**, *130*, 12815–12820.

(24) Lyu, L.-M.; Huang, M. H. *J. Phys. Chem. C* **2011**, *115*, 17768–17773.

(25) Zhang, Y.; Deng, B.; Zhang, T.; Gao, D.; Xu, A.-W. *J. Phys. Chem. C* **2010**, *114*, 5073–5079.